Epigenetic Repression of *microRNA-129-2* Leads to Overexpression of *SOX4* Oncogene in Endometrial Cancer

Yi-Wen Huang,[1] Joseph C. Liu,[1] Daniel E. Deatherage,[1] Jingqin Luo,[2] David G. Mutch,[3] Paul J. Goodfellow,[3,4] David S. Miller,[5] and Tim H-M. Huang[1]

[1]Human Cancer Genetics Program, Comprehensive Cancer Center, The Ohio State University, Columbus, Ohio; [2]Division of Biostatistics, [3]Department of Obstetrics and Gynecology, Division of Gynecologic Oncology, and [4]Department of Surgery, Washington University School of Medicine and Siteman Cancer Center, St. Louis, Missouri; and [5]Department of Obstetrics and Gynecology, UT Southwestern Medical Center at Dallas, Dallas, Texas

Abstract

Genetic amplification, mutation, and translocation are known to play a causal role in the upregulation of an oncogene in cancer cells. Here, we report an emerging role of microRNA, the epigenetic deregulation of which may also lead to this oncogenic activation. *SOX4*, an oncogene belonging to the SRY-related high mobility group box family, was found to be overexpressed ($P < 0.005$) in endometrial tumors ($n = 74$) compared with uninvolved controls ($n = 20$). This gene is computationally predicted to be the target of a microRNA, *miR-129-2*. When compared with the matched endometria, the expression of *miR-129-2* was lost in 27 of 31 primary endometrial tumors that also showed a concomitant gain of *SOX4* expression ($P < 0.001$). This inverse relationship is associated with hypermethylation of the *miR-129-2* CpG island, which was observed in endometrial cancer cell lines ($n = 6$) and 68% of 117 endometrioid endometrial tumors analyzed. Reactivation of *miR-129-2* in cancer cells by pharmacologic induction of histone acetylation and DNA demethylation resulted in decreased SOX4 expression. In addition, restoration of *miR-129-2* by cell transfection led to decreased SOX4 expression and reduced proliferation of cancer cells. Further analysis found a significant correlation of hypermethylated *miR-129-2* with microsatellite instability and *MLH1* methylation status ($P < 0.001$) and poor overall survival ($P < 0.039$) in patients. Therefore, these results imply that the aberrant expression of *SOX4* is, in part, caused by epigenetic repression of *miR-129-2* in endometrial cancer. Unlike the notion that promoter hypomethylation may upregulate an oncogene, we present a new paradigm in which hypermethylation-mediated silencing of a microRNA derepresses its oncogenic target in cancer cells. [Cancer Res 2009;69(23):9038–46]

Introduction

The *SRY-related high-mobility group box 4* gene, or *SOX4*, is known to be overexpressed in prostate, hepatocellular, lung, bladder, and medulloblastoma cancers with poor prognostic features and advanced disease status (1–6). Its oncogenic potentials have been shown in knock-in cells leading to aberrant transformation, whereas the proliferation and metastatic capability has been greatly reduced in knockout cancer cells (1–4, 7). Functional analysis has shown that SOX4 belongs to the T-cell factor/lymphoid enhancer factor family of transcription factors that mediate transcription responses to Wnt signaling (2, 8). More recently, a genome-wide chromatin immunoprecipitation study has further uncovered additional transcriptional targets of SOX4 that are associated with the transforming growth factor β, Hedgehog, and Notch pathways, microRNA (miRNA) processing, and tumor metastasis (7, 9).

Genetic mechanisms leading to aberrant expression of *SOX4* have been explored in cancer cells. *SOX4* is mapped to chromosome 6p22, a region frequently amplified in lung, bladder, and endometrial cancers (2, 10–12). Somatic mutations have also been found in the exon region of this intronless gene in lung cancer (2). However, there is no experimental evidence to show positive correlation between these reported genetic alterations and the aberrantly increased *SOX4*. One emerging mechanism is miRNA-mediated oncogene expression.

miRNAs, a class of small noncoding RNAs (18–25 nunleotides), are known to form imperfect paring at the 3′-end of untranslated regions (UTR) of a target locus, resulting in mRNA degradation or translational inhibition (13). Through this posttranscriptional regulatory mechanism, miRNAs control a variety of physiologic processes in normal cells, and deregulation of miRNAs may promote tumorigenesis (14). Increasing evidence indicates that epigenetic perturbations may contribute to abnormal miRNA expression in cancer cells (15). One well-studied epigenetic phenomenon is DNA methylation frequently observed in the promoter CpG island regions of genes (16). Whereas promoter hypermethylation is associated with transcriptional silencing of coding genes for tumor suppressor functions, promoter hypomethylation can be related to activation of oncogenes in cancer cells (16, 17). We therefore speculate whether methylation alteration may commonly occur in noncoding miRNAs, resulting in deregulation of its target genes in cancer cells.

Here, we report for the first time that the *SOX4* oncogene is also overexpressed in endometrial cancer. A miRNA, *miR-129-2*, was computationally predicted and functionally validated to be an upstream regulator of *SOX4*. A CpG island encompassing the *miR-129-2* locus was found to be hypermethylated in endometrial cancer cell lines and primary tumors. We further show that this methylation-mediated silencing has a causal role for *SOX4* activation in endometrial cancer.

Materials and Methods

Endometrial specimens and cell lines. Tissue specimens (117 tumors and 8 uninvolved controls) were obtained as part of our ongoing work on characterizing molecular alterations in endometrioid endometrial

Note: Supplementary data for this article are available at Cancer Research Online (http://cancerres.aacrjournals.org/).

Requests for reprints: Tim H-M. Huang, Human Cancer Genetics Program, The Ohio State University, 814 Biomedical Research Tower, 460 West 12th Avenue, Columbus, OH 43210. Phone: 614-688-8277; Fax: 614-292-5995; E-mail: tim.huang@osumc.edu.

doi:10.1158/0008-5472.CAN-09-1499

carcinomas. All participants consented to both molecular analyses and follow-up studies, and the protocols were approved by the Human Studies Committee at the Washington University and the Ohio State University. Clinicopathologic variables of tumors, including age, stage, grade, microsatellite instability (MSI), and *MLH1* methylation, were summarized in Supplementary Table S1 and reported in our previous study (18). Human endometrial cancer cell lines, AN3CA, HEC1A, Ishikawa, KLE, RL95-2, and SK-UT-1B, were routinely maintained in our laboratory (19), and ECC-1 cells were obtained from the American Type Culture Collection. For epigenetic studies, these cells were treated with 5-aza-2′-deoxycytidine (DAC; 0.5 μmol/L; Sigma) for 48 h and/or trichostatin A (TSA; 5 μmol/L; Sigma) for 24 h. DNA and RNA from treated and untreated cells were isolated using standard protocols (20).

Endometrial tissue microarray. Tissue microarray slides, each containing a total of 74 endometrial tumors and 20 normal specimens, were obtained from US Biomax. Patients' characteristics were summarized in Supplementary Table S2. These slides were preprocessed before immunohistostaining. Antigen retrieval was done by heat-induced epitope retrieval, in which the slides were placed in Dako TRS solution (pH 6.1) for 25 min at 94°C. Slides were then placed on a Dako autostainer with primary antibody (SOX4, 1:50; Abcam) and incubated for 60 min at room temperature. Staining was visualized with 3,3′-diaminobenzidine chromogen, and slides were then counterstained and dehydrated through graded ethanol solutions. Images were digitally scanned with iScan (BioImagene) and analyzed with the BioImagene TissueMine software for discriminating immunohistochemically stained cancer cells from the surrounding stromal tissue. Intensities of nuclear staining were measured as segmented images and then quantified. The algorithm reported the number and percentage of positively stained and nonstained nuclei.

Cell transfection. ECC-1 and Ishikawa cells (3×10^6) were transfected with mature *miR-129-2* mimics (*miR-129-3p* and *miR-129-5p*, 2.5 nmol/L; Ambion), pre-miR negative control (#1, 2.5 nmol/L; Ambion), *SOX4* siGenome SMART pool siRNA (2.5 nmol/L; Dharmacon), siGenome nontargeting siRNA pool (#1, 2.5 nmol/L; Dharmacon), and plasmids using the Cell Line Nucleofector Kit (Lonza) according to manufacturer's instructions.

Reverse transcription and quantitative PCR. Total RNA (1 μg) was reverse transcribed with the Superscript III reverse transcriptase (Invitrogen). PCR was done as described previously (20). Specific primers for amplification are listed in the Supplementary Table S3. The relative expression of a coding gene in cells was determined by comparing the threshold cycle (Ct) of the gene against the Ct of *GAPDH* (20).

For detecting mature miRNA molecules (i.e., *miR-129-3p* and *miR-129-5p*), reverse transcription was done following the Applied Biosystems TaqMan MicroRNA Assay protocol. This sensitive system has been designed to specifically detect mature miRNAs that are distinct from their precursors. In addition, the assay can often distinguish between miRNA targets that differ by only a single nucleotide (21). All reactions were done in triplicate. The expression of *miR-129-2-3p* or *miR-129-2-5p* was normalized using *RNU48* or *U6*. The expression relative to *RNU48* or *U6* was determined using the $2^{-\Delta Ct}$ method.

Western blot analysis. Whole-cell protein lysates were extracted with the M-PER Mammalian Protein Extraction Reagent (Pierce). Western blot analysis was conducted using antibodies against SOX4 (Abcam) and β-actin (Santa Cruz).

Cell proliferation assay. Cell proliferation was monitored using the CellTiter 96 Aqueous solution (Promega). Endometrial cancer cells (3,000 per well) transfected with *miR-129-2*, negative control miRNA, *SOX4* siRNA, or nontargeting siRNA pool were seeded in 96-well plates. Cell proliferation was documented every 24 h following the manufacturer's protocol. To measure cell proliferation, 20 μL of MTS labeling reagent were added to each well and incubated at 37°C for 1 h. Absorbance was measured at 490 nm in an ELISA reader (Molecular Devices).

3′-UTR reporter assay. The full-length 3′-UTRs of *SOX4* and *UBE2F*, generous gifts from Dr. Joan Massague, were cloned into the Psicheck 2 dual luciferase reporter vector (Promega). ECC-1 or Ishikawa cells were transfected with reporter constructs and *miR-129-2* and/or its antagomir targeting endogenous *miR-129-2* (Ambion). Cells were lysed at 24 h after transfection, and the ratio of *Renilla* to firefly luciferase was measured using the dual luciferase assay (Promega). Normalized *Renilla*-to-firefly ratios were determined in the presence or absence of *miR-129-2* inhibition on *SOX4* UTR luciferase activities.

Combined bisulfite restriction analysis. Genomic DNA (500 ng) was treated with sodium bisulfite using the EZ DNA Methylation kit (Zymo Reasearch) following the manufacturers' recommended protocols. Combined bisulfite restriction analysis (COBRA) was used to evaluate methylation of *miR-129-2*. Target sequences were amplified by PCR, and the products were digested with *Aci*I (New England Biolabs) to identify methylated sequences. Primer sequences and PCR conditions are presented in Supplementary Table S3. Digested and nondigested PCR products were resolved on 2% agarose gels stained with ethidium bromide. DNA fragments digested by *Aci*I were scored as "methylated" in a given sample.

MassARRAY analysis. To quantify methylation levels of the *miR-129-2* CpG islands in clinical samples, the high-throughput MassARRAY platform (Sequenom) was carried out as described previously (22). Briefly, bisulfite-treated DNA was amplified with primers for the *miR-129-2* CpG island. The PCR products were spotted on a 384-pad SpectroCHIP (Sequenom), followed by spectral acquisition on a MassARRAY Analyzer. Methylation data of individual units (one to three CpG sites per unit) were generated by the EpiTyper software (Sequenom).

Statistical and survival analyses. Student's *t* test or Wilcox test was used to compare the immunohistostaining, cell proliferation, and reverse transcription and quantitative PCR (RT-qPCR) results in different treatment groups. Significance was assigned at $P < 0.05$ (*). The relationship between methylation levels of *miR-129-2* and relevant categorical clinicopathologic covariates was done using the Wilcox rank sum test for binary variables. The Kruskal-Wallis test was used followed by a pairwise Wilcoxon rank sum test. Overall survival was defined as the time interval from the date of diagnosis to the date of death or latest follow-up if alive. Recurrence-free survival was defined as the time interval from surgery to recurrence, disease progression, or latest follow-up. The Kaplan-Meier product limit method was used to estimate the empirical survival functions for categorical covariates accompanied with *P* value from the log-rank test. Univariate Cox proportional hazard models were used to access the effect of a continuous covariate on survival outcomes. Multivariate Cox proportional hazard models were fitted to examine the potential predictive effect of covariates of interest on survival outcomes after adjustment for confounding factors. All tests were two-sided and all analyses were done using R.

Results

SOX4 is overexpressed in endometrioid endometrial carcinomas. To determine whether SOX4 is aberrantly expressed in endometrial tumors, we conducted tissue microarray analysis in a panel of 74 endometrioid endometrial carcinomas and 20 uninvolved controls (see representative immunohistostaining images in Fig. 1*A, left*). The nuclear staining intensities of SOX4 were significantly higher in tumor sections than those of normal tissue sections ($P < 0.005$; Fig. 1*A, right*). This finding is consistent with the RT-qPCR results in which the levels of *SOX4* mRNA were higher in tumors ($n = 31$) compared with the adjacent normal counterparts ($P < 0.001$; Fig. 2*D, left*).

In a knockout study, we assessed the role of SOX4 in endometrial cancer cells. ECC-1 and Ishikawa cells were transiently transfected with *SOX4* siRNA or a nontargeting control. Both protein and mRNA levels of SOX4 were found to be reduced to ≤50% in transfectants (Fig. 1*B* and *C*), resulting in attenuation of cell growth (Fig. 1*D*). This *SOX4* knockout, however, had no effects on cell invasion or migration (data not shown).

***miR-129-2* is a negative regulator of *SOX4*.** Because miRNA may have a potential role in mediating oncogene repression (14), we searched potential target sequences at the 3′-UTR of *SOX4*

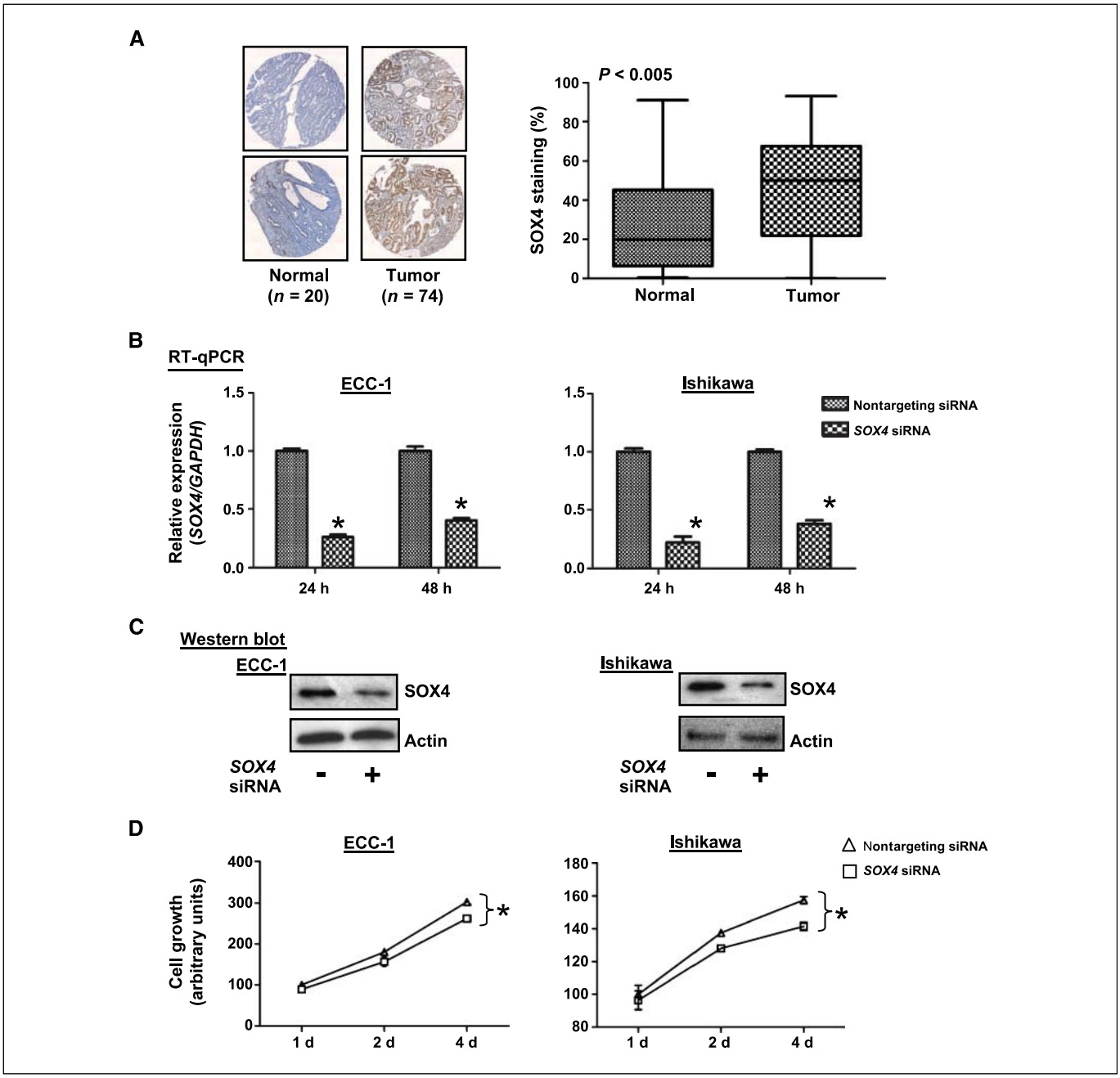

Figure 1. SOX4 is overexpressed in endometrial tumors. *A,* representative photographs of endometrial tissue microarrays (1.5 mm in core diameter) that were immunohistochemically stained for SOX4 and scored for nuclear staining by the TissueMine software. Box plots of SOX4 nuclear staining for normal tissue ($n = 20$) and endometrial tumors ($n = 74$); $P < 0.005$. *B* and *C,* relative expression levels of *SOX4* mRNA and protein in ECC-1 and Ishikawa cells after transient transfection with *SOX4* siRNA or a pool of nontargeting siRNA oligonucleotides for 24 and/or 48 h. *GAPDH* and β-actin served as internal controls for RT-qPCR and Western blotting, respectively. *Bars,* SD of triplicates; *, $P < 0.05$. *D,* cellular proliferation was measured by MTS assay in endometrial cancer cells transfected with *SOX4* siRNA or nontargeting siRNA. Transfectants (3,000 per well) were placed in 96-well plates and proliferation was measured every 24 h. *Points,* mean of at least three measurements. *, $P < 0.05$.

using three software programs: PicTar, TargetScan, and miRanda (23–25). Putative binding sites were found in a miRNA locus, *miR-129-2*, which is the precursor of two mature forms, *miR-129-3p* and *miR-129-5p* (Fig. 2*A* and *B*). To further validate this computational finding that *miR-129-2* may negatively regulate *SOX4*, we assessed the expression of 3′-UTR of *SOX4* in luciferase reporter assays (Fig. 2*C*). The expression of the *SOX4* reporter was significantly reduced to ≤55% in *miR-129-3p*– or *miR-129-5p*–transfected ECC-1 and Ishikawa cells, but not in control cells. Transfection with either miRNA did not affect the reporter activity of a negative control gene, *UBE2F*, which has no known *miR-129-2* binding sites on its UTR. Moreover, inhibition of *miR-129-3p* or *miR-129-5p* by antagomirs slightly enhanced the expression of *SOX4*, suggesting that this gene is a direct target of *miR-129-2*. We additionally confirmed this inverse relationship between *miR-129-3p* and *SOX4* mRNA and expression using the aforementioned 31 paired samples (Fig. 2*D*).

Methylation-mediated silencing of *miR-129-2* derepresses SOX4 expression. Because the expression of *miR-129-2* is frequently lost in endometrial tumors (see Fig. 2*D*) and the 5′-end of this locus has a canonical CpG island (Fig. 3*A*), we determined whether this downregulation is mediated by epigenetic mechanisms. Hypermethylation of this promoter CpG island was detected in six endometrial cancer cell lines, ECC-1, HEC1A, Ishikawa, KLE, RL95-2, and SK-UT-1B, based on a COBRA assay (Fig. 3*B*). When these cells were treated with a demethylating agent, DAC (0.5 μmol/L), a histone deacetylase inhibitor, TSA (5 μmol/L), or their combination, reactivation of *miR-129-3p* was observed in four (Ishikawa, KLE, RL95-2, and SK-UT-1B) of the six cell lines analyzed that were treated with DAC (Fig. 3*C*). More profound effects of this reexpression were found in all these cell lines treated with TSA and the combination (Fig. 3*C*; Supplementary Fig. S1). These results suggest that the loss of *miR-129-2* expression is associated with promoter hypermethylation in endometrial cancer cells. Interestingly, these epigenetic treatments might lead to the suppression of SOX4 in endometrial cancer cells. The effect occurred at the mRNA level in ECC-1, HEC1A, KLE, RL95-2, and SK-UT-1B cells

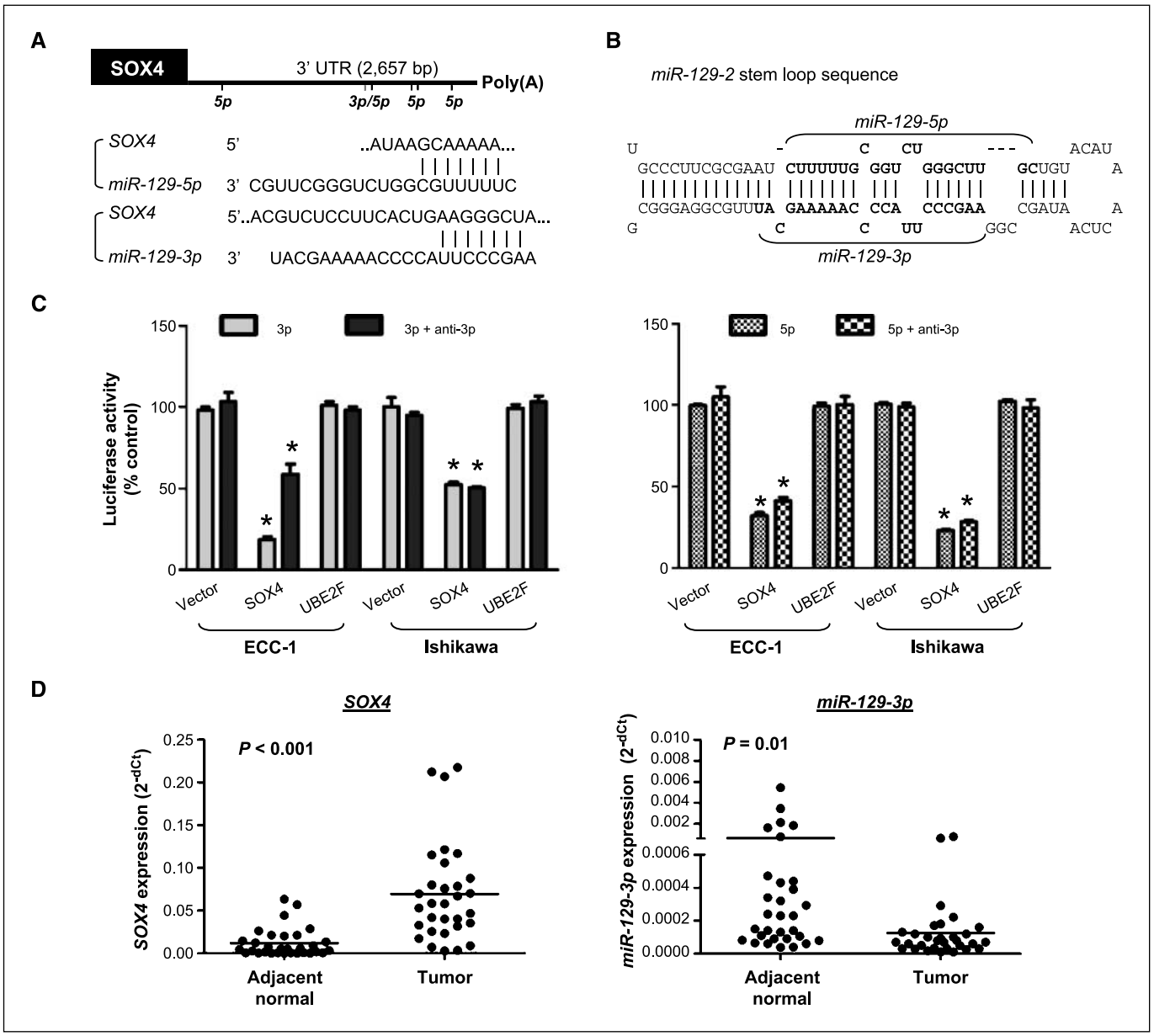

Figure 2. *miR-129-2* directly targets *SOX4. A,* bioinformatic analysis of *miR-129-3* and *miR-129-5p* (the mature forms of *miR-129-2*) predicted binding sites in the *SOX4* 3′-UTR (*bars under line*). The predicted pairing of mRNA target region (*top*) and miRNA (*bottom*) is as indicted, where a line indicates hydrogen bonding. *B,* predicted secondary structure of *miR-129-2*. The stem loop structure of *miR-129-2* is a precursor to two mature miRNAs, *miR-129-3p* and *miR-129-5p* (*bold text*). *C, miR-129-3p* and *miR-129-5p* suppressed the expression of a luciferase vector with the *SOX4* 3′-UTR. A luciferase expression vector with the 3′-UTR of *SOX4* and *UBE2F* or an empty vector was transfected into ECC-1 and Ishikawa cells. At the same time, anti–*miR-129-3p* or anti–*miR-129-5p* (*anti-3p* or *anti-5p*) and/or *miR-129-3p* or *miR-129-5p* (*3p* or *5p*) were introduced. Twenty-four hours after the transfection, the cells were harvested and assayed for luciferase activity. *Renilla* luciferase was used for normalization to empty vector for the transfection efficiency. *Bars,* SD. *, $P < 0.05$, compared with empty vector. *D,* dot plots showing an inverse relationship between *SOX4* (*left*) and *miR-129-3p* (*right*) mRNA expression in 31 pairs of endometrial tumors and adjacent normal tissues. *Horizontal bars,* mean expression levels. Significant differences were determined using Student's *t* tests.

(Fig. 3*D, left*). This suppression, however, was more prominent at the posttranslational level for Ishikawa and RL95-2 cells (Fig. 3*D, right*). In addition, we showed that the expression of four other *miR-129-2* targets, *EIF2C3, PLCG1, RAB21*, and *STAT5B*, was repressed in cancer cells treated with DAC and/or TSA (Supplementary Fig. S2). Taken together, the observation indirectly indicates that these epigenetic treatments may lead to reactivation of *miR-129-2*, which in turn represses the expression of *SOX4*.

To further prove this inverse relationship, we conducted a functional knock-in study in two endometrial cell lines, ECC-1 and Ishikawa, harboring the epigenetically silenced *miR-129-2*. Transient transfection of these cells with either *miR-129-3p* or *miR-129-5p* resulted in reduction of both *SOX4* mRNA and protein (Fig. 4*A* and *B*) (Note: Transfection efficiency was examined by measuring each mature miRNA; see Supplementary Fig. S3.) Moreover, the knock-in of one of these mimics, *miR-129-5p*, greatly reduced the proliferation of these cancer cells ($P < 0.05$; Fig. 4*C*). In addition, the expression of three SOX4-regulated genes (*DHX9, FZD5*, and *SEMA3C*; refs. 3, 9) was partially reduced in ECC-1 cells treated with DAC and/or TSA or ectopically transfected with *miR-129-3p* or *miR-129-5p* (Supplementary Fig. S4). Taken together, these *in vitro* studies suggest that *miR-129-2* negatively regulates

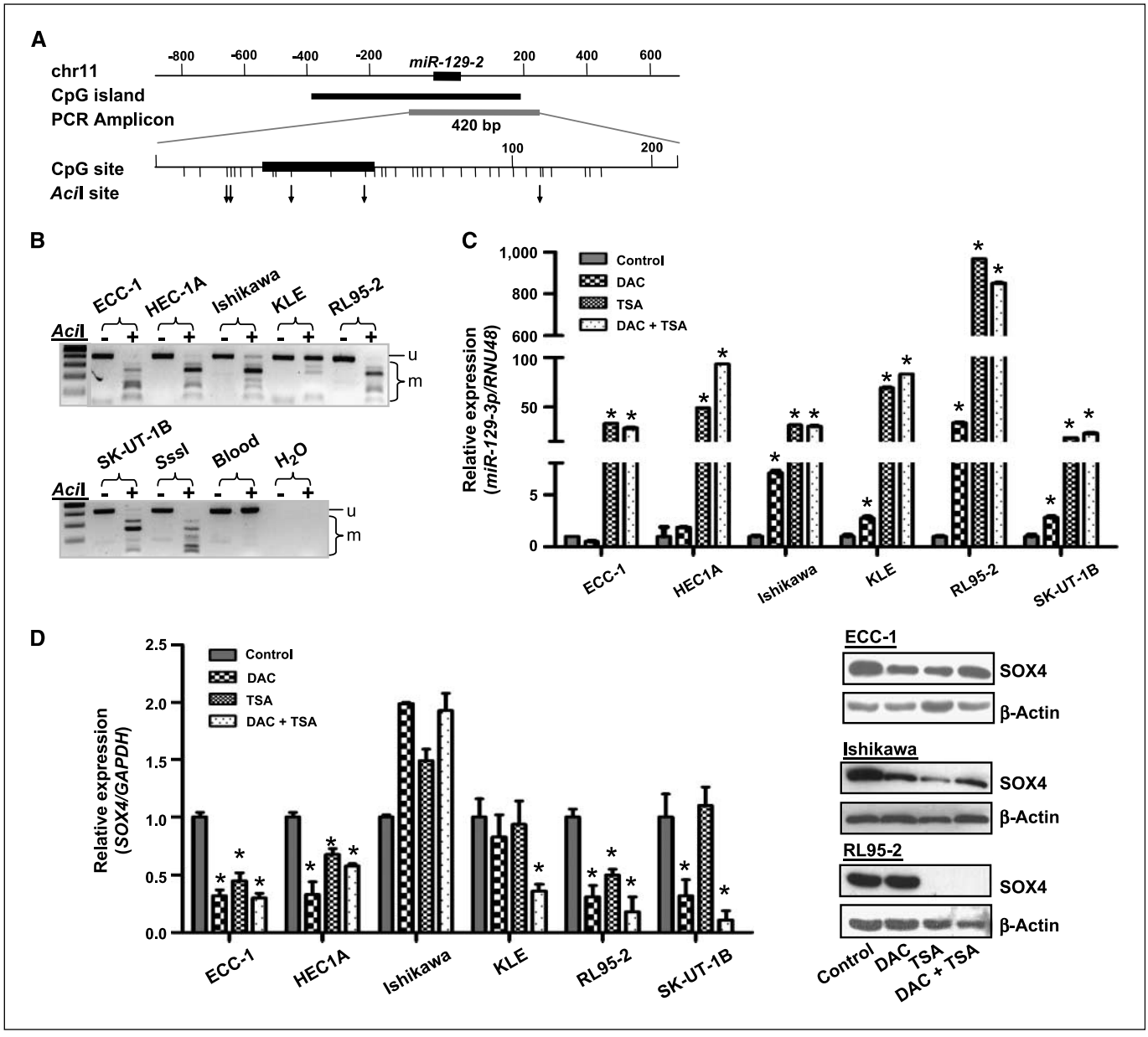

Figure 3. Reactivation of *miR-129-2* in cancer cells by pharmacologic induction of hyperacetylation and DNA demethylation leads to reduced *SOX4* expression at both the mRNA and protein levels. *A,* genomic map of *miR-129-2* CpG island and amplicon. *Bar under line,* CpG site; ↓, *Aci*I cutting sites. *B,* COBRA analysis in endometrial cancer cell lines. *u,* unmethylated band; *m,* methylated bands; *Sss*I, 100% methylated control; *Blood,* a mix of four normal peripheral blood samples as negative control; +, *Aci*I restriction enzyme added; –, without *Aci*I. *C,* the relative expression levels of *miR-129-3p* in endometrial cancer cell lines treated with DAC and/or TSA in relation to untreated controls were determined by RT-qPCR analysis. *RNU48* was used as internal control gene. *Bar,* SD; *, $P < 0.05$, compared with untreated control of the same cell type. *D,* relative expression levels of *SOX4* mRNA (*left*) and protein (*right*) indicating a downregulation of SOX4 in endometrial cancer cells after treatment with DAC and/or TSA. *GAPDH* or β-actin was used as internal or loading control, respectively.

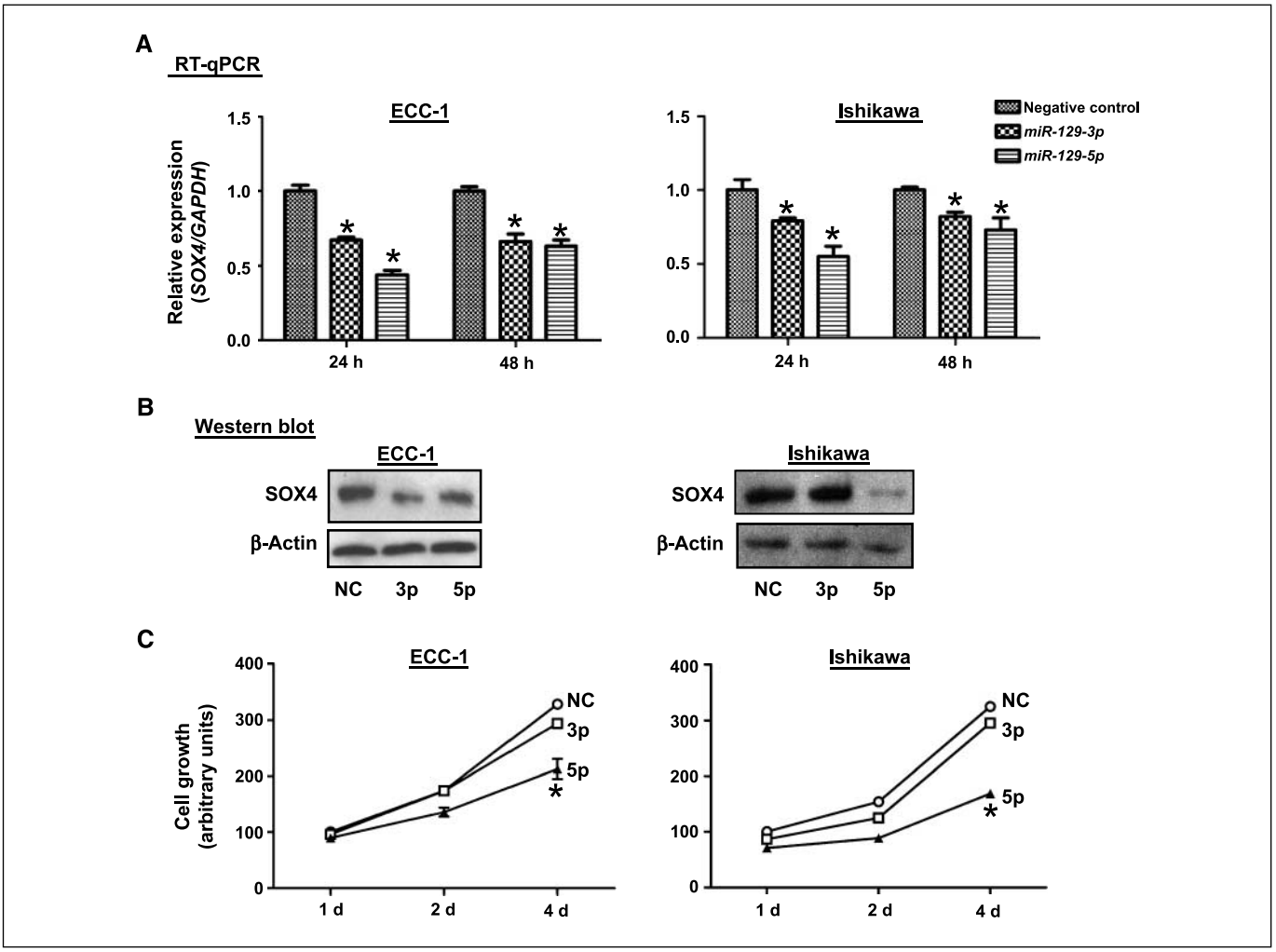

Figure 4. Functional analysis of *miR-129-2* in endometrial cancer cell lines. *A* and *B*, relative levels of *SOX4* mRNA (*A*) or protein (*B*) expression in ECC-1 and Ishikawa cells after transient transfection with miRNAs or negative control (*NC*) RNA oligonucleotides for 24 or 48 h. *GAPDH* or β-actin served as an internal control of mRNA or protein, respectively. *Bars*, SD from triplicates; *, $P < 0.05$, compared with negative control at the same time point. *C*, cellular proliferation by MTS assay in the endometrial cancer cell lines ECC-1 and Ishikawa transfected with *miR-129-3p* (*3p*), *miR-129-5p* (*5p*), or negative control. Proliferation was measured as described in Fig. 1*C*.

SOX4 and that promoter hypermethylation of this miRNA derepresses its expression.

Hypermethylation of *miR-129-2* is associated with shorter patient survival, MSI, and *MLH1* methylation in endometrial tumors. To confirm our *in vitro* findings in primary tumors, we first studied the methylation patterns of the *miR-129-2* CpG island (see Fig. 3*A*) in eight tumors with matched normal endometria by COBRA and quantitative MassARRAY. We showed that the tumors were hypermethylated compared with the corresponding adjacent normal tissues (Supplementary Fig. S5). We then extended this methylation study to 117 (34 recurrent and 83 nonrecurrent) primary endometrioid endometrial tumors and 8 uninvolved controls. Quantitative analysis indicated that 80 of these primary tumors exhibited extensive methylation in 14 units (one to three CpG sites per unit) of the *miR-129-2* CpG island relative to those of uninvolved controls ($P < 0.0005$; Fig. 5*A*). This methylation survey in the patient cohort also uncovered a pattern in which methylation accumulation may begin at the flanking regions and progressively invade to the core of this CpG island, consistent with the so-called methylation spread theory (26).

The mean methylation level of each CpG unit was used to compare between the recurrent and nonrecurrent groups. More accumulation of *miR-129-2* methylation was found in the former group, but the sample size of this cohort could be too small to reach statistical significance ($P = 0.066$; Fig. 4*B*). Detailed analysis of individual CpG units is shown in Supplementary Fig. S6. We also evaluated the association between *miR-129-2* hypermethylation and patient survival. On univariate analysis, *miR-129-2* hypermethylation was correlated with shorter overall survival (Cox hazard ratio, 1.02; $P = 0.018$), but not with recurrence-free survival (Cox hazard ratio, 1.02; $P = 0.067$), when the mean methylation level of normal controls was used to set the threshold. The Kaplan-Meier survival analysis indicated that patients with this hypermethylation had poor overall survival (Fig. 5*C*; $P = 0.039$, log-rank test). Statistical analysis further revealed that *miR-129-2* hypermethylation was significantly associated with MSI and *MLH1* methylation ($P < 0.0001$; Fig. 5*D*). Endometrial tumors exhibiting the MSI phenotype usually have high replication error rates and genomic instability (18, 27). This defect is attributed, in part, to epigenetic repression of *MLH1*, which is responsible for DNA mismatch repair in normal cells (27).

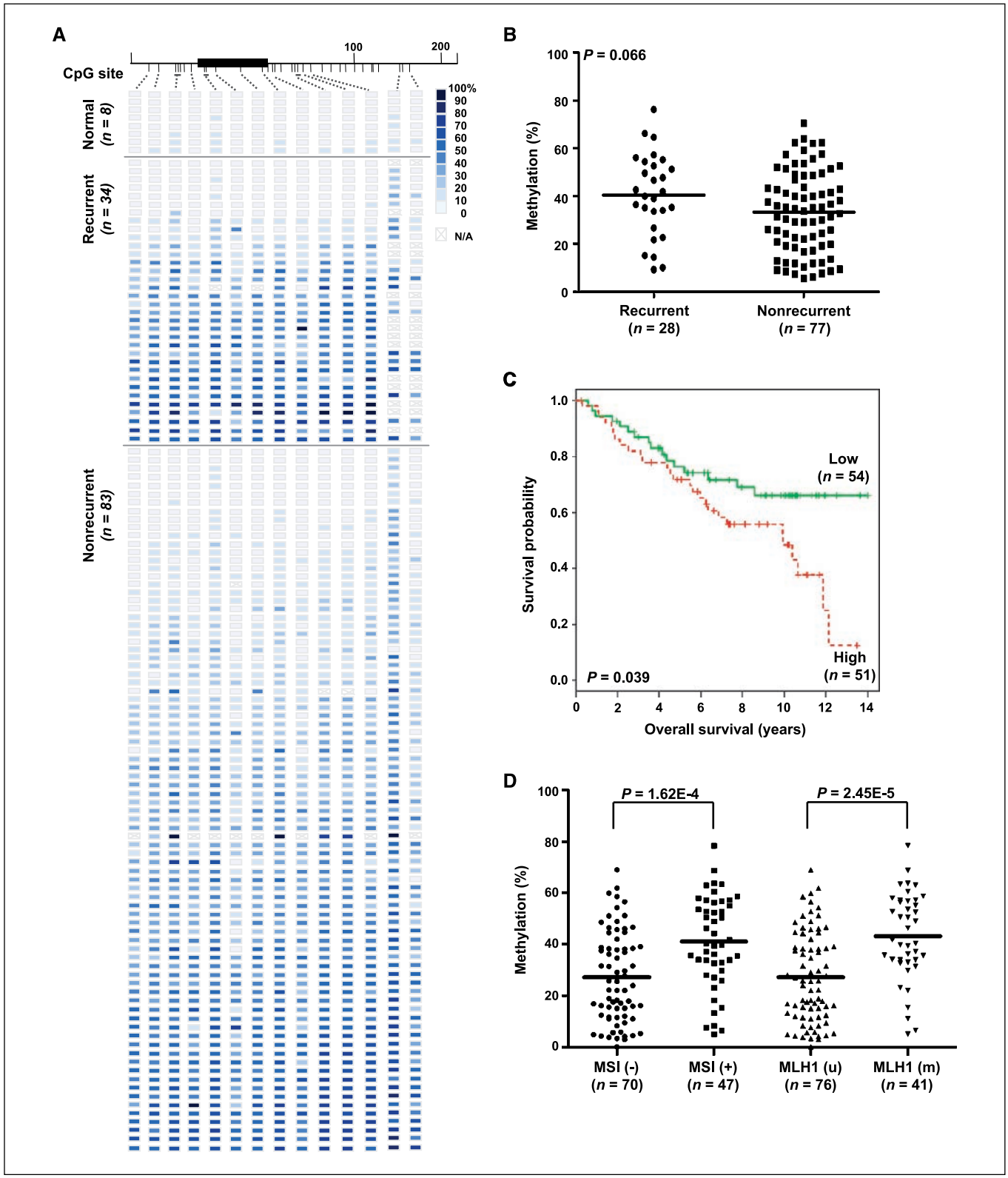

Figure 5. Methylation of *miR-129-2* CpG island and clinicopathologic covariate analyses in primary endometrioid endometrial tumors. *A,* methylation profiles of 8 normal endometrial tissues and 34 recurrent and 83 nonrecurrent primary tumors, created following MassARRAY analysis. Each row represents a sample, and each column represents a CpG unit. Color coding depicts the degree of methylation, with dark blue being 100% and white being 0%. *N/A,* not analyzable. *B,* dot plots show that *miR-129-2* hypermethylation is moderately correlated with recurrent diseases. The mean of normal specimens in *A* was set as a threshold for analysis. *Dots,* mean of each specimen on the first five CpG sites in *A. Horizontal lines,* mean values. *P* value was calculated by Wilcox test. *C,* Kaplan-Meier curves for overall survival. Samples were grouped according to the mean level of methylation for the first five CpG units of *miR-129-2*, when the mean exceeded the mean of normal specimens. *Vertical bars,* excluded cases. *P* value estimated from log-rank test. *D,* dot plots indicating that the level of *miR-129-2* promoter methylation is positively correlated with MSI and *MLH1* methylation status.

Discussion

In addition to genetic alterations, promoter hypomethylation has been recognized as an epigenetic mechanism that contributes to oncogene activation in cancer cells (16, 17). In this case, a demethylation event is supposed to occur in an inactive, methylated promoter, leading to transcriptional reactivation of an oncogene. However, experimental proof for genuine promoter hypomethylation is frequently difficult and inconclusive because the outgrowth of a subpopulation of cancer cells may confound this epigenetic observation. For example, the oncogene of interest may have never been silent in a minor population of cancer-initiating cells, whereas the majority of other cells display promoter hypermethylation of the gene. The increased expression of this oncogene may simply result from rapid expansion of these few cells that eventually take over the whole population during tumor progression. If this scenario indeed occurs, it cannot be a bona fide epigenetic event for oncogene activation.

In this study, we show that promoter hypermethylation can be directly associated with the activation of an oncogene. Specifically, this epigenetic event occurs in an upstream regulator, *miR-129-2*, which was shown to negatively regulate *SOX4* oncogene in both knock-in and knockout assays. *miR-129-2* is embedded in a canonical CpG island on chromosome 11, which was found to be frequently hypermethylated in endometrial cancer. This epigenetic event results in *miR-129-2* silencing, which in turn derepresses *SOX4* expression. Although we still cannot rule out hypomethylation of the *SOX4* promoter CpG island as one of the causes, our present observation conclusively suggests that promoter hypermethylation of *miR-129-2* is a common mechanism leading to the *SOX4* overexpression in endometrial cancer.

It should be noted that a second CpG island is found 1.2 kb upstream from the first one analyzed in this study. In addition, the 5′-ends of two transcripts, *BG120451* and *BI964058*, are located in this upstream region. It is possible that these transcripts are the primary RNAs for *miR-129-2* (28). Future mapping of putative transcription start sites located in these 5′-end areas will provide insight into the transcriptional control of this miRNA locus. Additional methylation analysis may further determine the role of this second CpG island in the silencing of *miR-129-2* during endometrial tumorigenesis.

We have additionally searched the miRBase database and found that the expression of *SOX4* may be regulated by at least 16 putative miRNAs, including *miR-129-1* located on chromosome 7. Similar to *miR-129-2*, the *miR-129-1* precursor produces mature *miR-129-5p*, which negatively regulates SOX4, as described in this study. Because there is no known CpG island located near or within the *miR-129-1* locus, it remains to be determined whether this miRNA is transcriptionally silenced by other epigenetic mechanisms (e.g., EZH2-mediated histone modifications; ref. 29) in endometrial cancer.

Five (*miR-203, miR-335, miR-219-2, miR-596*, and *miR-618*) of the other 15 miRNAs are located close to CpG islands based on our computational analysis (data not shown). Among these loci, *miR-335* is the only one currently reported to be lost in primary breast tumors of recurrent patients (7). However, it remains to be determined whether promoter hypermethylation plays a role in the silencing of this locus. Future studies will therefore be important to study the coordinate regulation of these miRNAs on *SOX4* repression. It is also possible that concurrent hypermethylation of these loci contributes to a CpG island methylator phenotype (30) and may improve the statistical power for predicting disease recurrence in our endometrial patient cohort (see Fig. 5*B*).

Extending from our present observation, epigenetically mediated silencing of other miRNAs that lead to tumor progression has recently been reported in the literature (15, 31–33). For example, *ABL1* was showed to be a direct target of *miR-203* (32). This miRNA was genetically and epigenetically downregulated in leukemia cells expressing ABL1 or BCR-ABL1 fusion protein (32). Restoration of *miR-203 in vitro* led to reduced *ABL1* and *BCR-ABL1* expression and decreased proliferation of malignant cells (32). Taken together, these and our studies clearly indicate that epigenetic silencing of tumor-suppressive miRNAs can be an important constituent in cancer epigenomes and that the event is as significant as hypomethylation of oncogenes and hypermethylation of tumor suppressor genes.

In conclusion, our findings support a comprehensive screening of miRNA regulators at the 3′-UTR regions of all known oncogenes. High-throughout functional studies can be developed to establish the inverse relationship between these tumor-suppressive miRNA loci and their target oncogenes. This type of omics study may find that epigenetically mediated silencing of these miRNAs can be as common as genetic alterations that contribute to oncogene activation in cancer cells. As such, the combined epigenetic and miRNA-based therapies can be feasible options for future treatments in cancer patients.

Disclosure of Potential Conflicts of Interest

All authors have no potential conflicts of interest.

Acknowledgments

Received 4/23/09; revised 7/29/09; accepted 9/22/09; published OnlineFirst 11/3/09.

Grant support: NIH grants R01 CA069065, U01 ES015986, and U54 CA113001 (T.H-M. Huang); NIH grants R01 CA071754 and P50 CA134254 (P.J. Goodfellow); and funds from the Ohio State University Comprehensive Cancer Center (T.H-M. Huang).

The costs of publication of this article were defrayed in part by the payment of page charges. This article must therefore be hereby marked *advertisement* in accordance with 18 U.S.C. Section 1734 solely to indicate this fact.

We thank Chieh Ti Kuo, Xiao-Hong Gu, Geoffrey Tsoi, Mary Ann Mallon, and Drs. Kurtis H. Yearsley and Yu-I Weng for their technical assistance, and Drs. Joan Massague and Sohail F. Tavazoie (Memorial Sloan-Kettering Cancer Center, New York, NY) for providing *SOX4* and *UBE2F* 3′-UTR plasmids.

References

1. Pramoonjago P, Baras AS, Moskaluk CA. Knockdown of Sox4 expression by RNAi induces apoptosis in ACC3 cells. Oncogene 2006;25:5626–39.
2. Medina PP, Castillo SD, Blanco S, et al. The Sry-HMG box gene, SOX4, is a target of gene amplification at chromosome 6p in lung cancer. Hum Mol Genet 2009;18:1343–52.
3. Liao YL, Sun YM, Chau GY, et al. Identification of SOX4 target genes using phylogenetic footprinting-based prediction from expression microarrays suggests that overexpression of SOX4 potentiates metastasis in hepatocellular carcinoma. Oncogene 2008;27:5578–89.
4. Liu P, Ramachandran S, Ali Seyed M, et al. Sex-determining region Y box 4 is a transforming oncogene in human prostate cancer cells. Cancer Res 2006;66:4011–9.
5. Aaboe M, Birkenkamp-Demtroder K, Wiuf C, et al. SOX4 expression in bladder carcinoma: clinical aspects and *in vitro* functional characterization. Cancer Res 2006;66:3434–42.
6. Neben K, Korshunov A, Benner A, et al. Microarray-based screening for molecular markers in medulloblastoma revealed STK15 as independent predictor for survival. Cancer Res 2004;64:3103–11.
7. Tavazoie SF, Alarcon C, Oskarsson T, et al. Endogenous human microRNAs that suppress breast cancer metastasis. Nature 2008;451:147–52.
8. Sinner D, Kordich JJ, Spence JR, et al. Sox17 and Sox4 differentially regulate β-catenin/T-cell factor activity and proliferation of colon carcinoma cells. Mol Cell Biol 2007;27:7802–15.

9. Scharer CD, McCabe CD, Ali-Seyed M, Berger MF, Bulyk ML, Moreno CS. Genome-wide promoter analysis of the SOX4 transcriptional network in prostate cancer cells. Cancer Res 2009;69:709–17.
10. Hurst CD, Fiegler H, Carr P, Williams S, Carter NP, Knowles MA. High-resolution analysis of genomic copy number alterations in bladder cancer by microarray-based comparative genomic hybridization. Oncogene 2004;23:2250–63.
11. Levan K, Partheen K, Osterberg L, Helou K, Horvath G. Chromosomal alterations in 98 endometrioid adenocarcinomas analyzed with comparative genomic hybridization. Cytogenet Genome Res 2006;115:16–22.
12. Heidenblad M, Lindgren D, Jonson T, et al. Tiling resolution array CGH and high density expression profiling of urothelial carcinomas delineate genomic amplicons and candidate target genes specific for advanced tumors. BMC Med Genomics 2008;1:3.
13. Bartel DP. MicroRNAs: genomics, biogenesis, mechanism, and function. Cell 2004;116:281–97.
14. Calin GA, Croce CM. MicroRNA signatures in human cancers. Nat Rev Cancer 2006;6:857–66.
15. Saito Y, Liang G, Egger G, et al. Specific activation of microRNA-127 with downregulation of the proto-oncogene BCL6 by chromatin-modifying drugs in human cancer cells. Cancer Cell 2006;9:435–43.
16. Jones PA, Baylin SB. The epigenomics of cancer. Cell 2007;128:683–92.
17. Baylin SB, Ohm JE. Epigenetic gene silencing in cancer—a mechanism for early oncogenic pathway addiction? Nat Rev Cancer 2006;6:107–16.
18. Zighelboim I, Goodfellow PJ, Gao F, et al. Microsatellite instability and epigenetic inactivation of MLH1 and outcome of patients with endometrial carcinomas of the endometrioid type. J Clin Oncol 2007;25:2042–8.
19. Byron SA, Gartside MG, Wellens CL, et al. Inhibition of activated fibroblast growth factor receptor 2 in endometrial cancer cells induces cell death despite PTEN abrogation. Cancer Res 2008;68:6902–7.
20. Cheng ASL, Jin VX, Fan M, et al. Combinatorial analysis of transcription factor partners reveals recruitment of c-Myc to estrogen receptor-a responsive promoters. Mol Cell 2006;21:393–404.
21. Chen C, Ridzon DA, Broomer AJ, et al. Real-time quantification of microRNAs by stem-loop RT-PCR. Nucleic Acids Res 2005;33:e179.
22. Lin H-JL, Zuo T, Lin C-H, et al. Breast cancer-associated fibroblasts confer AKT1-mediated epigenetic silencing of cystatin M in epithelial cells. Cancer Res 2008;68:10257–66.
23. John B, Enright AJ, Aravin A, Tuschl T, Sander C, Marks DS. Human microRNA targets. PLoS Biol 2004;2:e363.
24. Lewis BP, Jones-Rhoades MW, Bartel DP, Burge CB. Prediction of mammalian microRNA targets. Cell 2003;115:787–98.
25. Krek A, Grun D, Poy MN, et al. Combinatorial microRNA target predictions. Nat Genet 2005;37:495–500.
26. Stirzaker C, Song JZ, Davidson B, Clark SJ. Transcriptional gene silencing promotes DNA hypermethylation through a sequential change in chromatin modifications in cancer cells. Cancer Res 2004;64:3871–7.
27. Laghi L, Bianchi P, Malesci A. Differences and evolution of the methods for the assessment of microsatellite instability. Oncogene 2008;27:6313–21.
28. Marson A, Levine SS, Cole MF, et al. Connecting microRNA genes to the core transcriptional regulatory circuitry of embryonic stem cells. Cell 2008;134:521–33.
29. Kondo Y, Shen L, Cheng AS, et al. Gene silencing in cancer by histone H3 lysine 27 trimethylation independent of promoter DNA methylation. Nat Genet 2008;40:741–50.
30. Toyota M, Ahuja N, Ohe-Toyota M, Herman JG, Baylin SB, Issa J-P. CpG island methylator phenotype in colorectal cancer. Proc Natl Acad Sci U S A 1999;96:8681–6.
31. Lujambio A, Ropero S, Ballestar E, et al. Genetic unmasking of an epigenetically silenced microRNA in human cancer cells. Cancer Res 2007;67:1424–9.
32. Bueno MJ, Pérez de Castro I, Gómez de Cedrón M, et al. Genetic and epigenetic silencing of microRNA-203 enhances ABL1 and BCR-ABL1 oncogene expression. Cancer Cell 2008;13:496–506.
33. Kozaki K-i, Imoto I, Mogi S, Omura K, Inazawa J. Exploration of tumor-suppressive microRNAs silenced by DNA hypermethylation in oral cancer. Cancer Res 2008;68:2094–105.